Effect of Mobile Phase Composition on Henry's Constants of 2-Amino-3-phenyl-propanoic Acid, 2-Amino-3-(3-indolyl)-propanoic Acid, and 2-Amino-3-(4-hydroxyphenyl)-propanoic Acid in a Capcell Pak C_{18} Chromatography

Qiao Han, Chang Geun Yoo, Se-Hee Jo, Sung Chul Yi,* and Sungyong Mun*

Department of Chemical Engineering, Hanyang University, Seoul, 133-791, Korea

The adsorption equilibria necessary for the design of a chromatographic process for amino acids separation were measured on a Capcell Pak C_{18} resin using a dynamic frontal analysis method. The single-component adsorption data of 2-amino-3-phenyl-propanoic acid, 2-amino-3-(3-indolyl)-propanoic acid, and 2-amino-3-(4-hydroxyphenyl)-propanoic acid were obtained at room temperature while varying the methanol content in the mobile phase from 5 % (v/v) to 70 % (v/v). On the basis of the resultant adsorption data, the Henry's constant, which is the ratio of solid-phase and liquid-phase concentrations at equilibrium, was determined for each amino acid and each mobile-phase composition. There was a large difference in Henry's constant among the three amino acids investigated. In addition, the Henry's constant of each amino acid showed a significant dependence on the mobile-phase composition. To correlate such a behavior, several models were tested. It was found that Abel's model containing three parameters was the most successful in correlating the Henry's constant of each amino acid as a function of mobile-phase composition. The data and model parameters reported in this study can be of use to the design of a chromatographic separation process based on a solvent gradient operation mode.

Introduction

Amino acids are vital biochemicals for protein synthesis and metabolism regulation.[1] Until now, various kinds of amino acids have been discovered. Some of them can be produced by the human body, while others named essential amino acids must be taken from outside artificially.[2] Among these essential amino acids, the following three (2-amino-3-phenyl-propanoic acid, 2-amino-3-(3-indolyl)-propanoic acid, and 2-amino-3-(4-hydroxyphenyl)-propanoic acid) are of noteworthy applications in the food or pharmaceutical industry.[3−7] 2-Amino-3-phenyl-propanoic acid (or phenylalanine) is used as a sweetener in place of sugar.[3] It is also effective in improving the recovery of taxol,[4] which is one of the well-known anticancer drugs. 2-Amino-3-(3-indolyl)-propanoic acid (or tryptophan) functions as a dietary supplement, as an effective sleep aid, and particularly shows considerable promise as an antidepressant.[5,6] 2-Amino-3-(4-hydroxyphenyl)-propanoic acid (or tyrosine) serves as a starting material of neurotransmitters.[7] Such importance of amino acids causes a large demand in industrial production of amino acids, which in turn requires a large-scale amino acid separation process. Conventionally, amino acids separation in an industrial scale is performed by fixed bed batch chromatography.[8] However, it is the commonly accepted fact that batch chromatography has low separation performance, i.e., low throughput, high solvent consumption, and low yield.[9,10] One of the ways to improve the performance of such a chromatographic process for amino acids separation is the introduction of solvent gradient simulated moving bed (SMB) chromatography,[11,12] which is a well-defined continuous separation process based on a change in mobile-phase composition along the bed. The economical merits of a solvent gradient SMB over a classical SMB and a batch chromatographic process have been verified in many previous studies.[11,12]

For successful application of the aforementioned solvent gradient SMB, the selection of a proper adsorbent is of importance. First of all, for the amino acids of interest, the adsorbent should create a widely varying adsorption affinity (i.e., Henry's constant) under a given range of mobile phase compositions. In addition, such a varying adsorption affinity of amino acids should be described using a proper model, which is to be incorporated into the design equation for solvent gradient SMB.[12]

Since the mobile-phase composition varies during the entire operation, the adsorbent should have a sufficient durability to withstand the harsh mobile-phase condition. One such durable adsorbent is a Capcell Pak C_{18} resin, which is manufactured by coating high-purity silica with silicone polymer through the vapor deposition method.[13] According to the literature and the manufacturer, the Capcell Pak C_{18} resin is very effective in suppressing the undesirable peak tailing phenomenon, and it can also cover a wide range of mobile phase compositions due to the polymer coating.[13]

The feasibility of using the Capcell Pak C_{18} resin as an adsorbent of solvent gradient SMB for amino acids separation will be explored in this study. For such purposes, the adsorption equilibria of 2-amino-3-phenyl-propanoic acid, 2-amino-3-(3-indolyl)-propanoic acid, and 2-amino-3-(4-hydroxyphenyl)-propanoic acid on the Capcell Pak C_{18} resin will be measured while varying mobile-phase composition. From the measured equilibrium data, the Henry's constants of the three amino acids will be estimated. Finally, the best model equation and its related

* Corresponding authors. Sungyong Mun. Tel.: +82-2-2220-0483. Fax: +82-2-2298-4101. E-mail: munsy@hanyang.ac.kr. Sung Chul Yi. Tel.: +82-2-2220-0481. Fax: +82-2-2298-4101. E-mail: scyi@hanyang.ac.kr.

10.1021/je800510y CCC: $40.75
Published on Web 10/07/2008

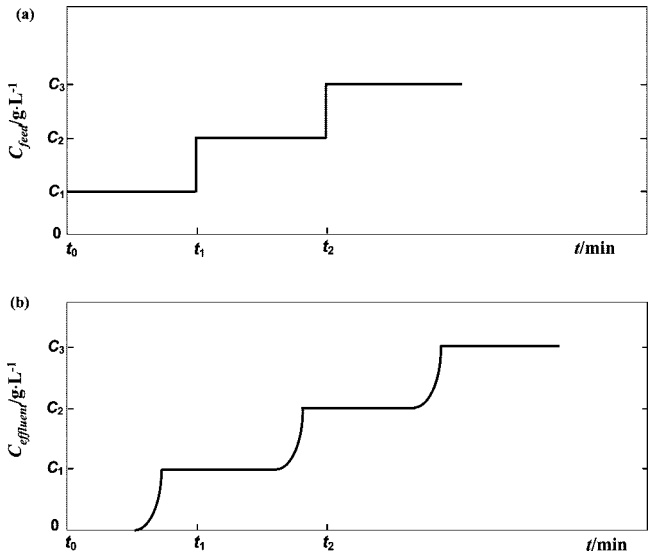

Figure 1. Schematic diagram of the concentration profiles at the column inlet and outlet for the case of a staircase frontal analysis method. (a) The profile of feed concentration C_{feed} as a function of time t at the column inlet. (b) The profile of effluent concentration C_{effluent} as a function of time t at the column outlet. x-axis labels: t_j, starting time of the $(j + 1)$th step. y-axis labels: C_j, feed concentrations employed during the jth step.

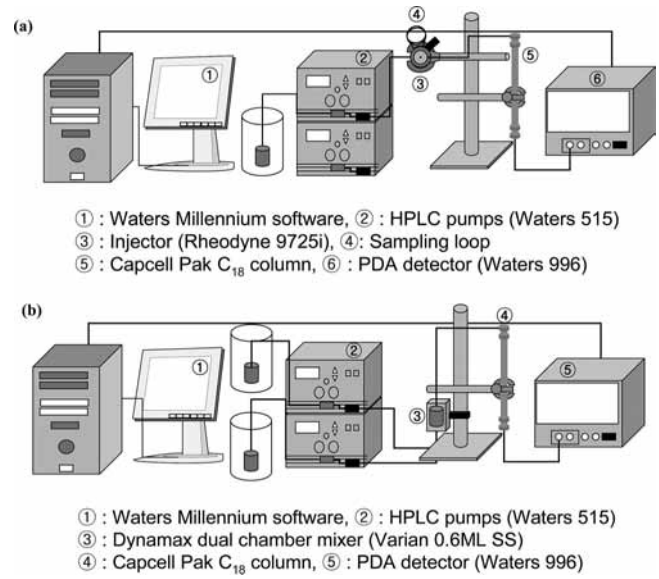

Figure 2. Schematic diagram of the experimental systems used in this study. (a) Experimental system for pulse tests. (b) Experimental system for staircase frontal tests.

coefficient values will be determined, which can allow an accurate prediction of the Henry's constant as a function of mobile-phase composition.

For the measurement of adsorption equilibria, several methods have been developed previously, and they were explained in detail elsewhere.[14−16] The methods have been commonly divided into (1) static method and (2) dynamic chromatographic method. Between the two, the dynamic chromatographic method is more efficient in terms of measurement time.[14,15] Furthermore, this method can be a much more appropriate one, if the measured equilibrium data are to be used in the design of a chromatographic separation process.[16] There have been several dynamic chromatographic methods available in the literature. Among them, a frontal analysis method was reported to have the highest accuracy.[14,16] Hence, all the adsorption equilibrium data of this study will be measured using a frontal analysis method.

The range of amino acids studied in this paper does not cover the whole amino acids available in nature. Only the aforementioned three amino acids (2-amino-3-phenyl-propanoic acid, 2-amino-3-(3-indolyl)-propanoic acid, and 2-amino-3-(4-hydroxyphenyl)-propanoic acid), which were reported to have valuable applications in industry, will be studied.

Theory

Determination of Adsorption Isotherms by Frontal Analysis. One of the popular methods for measuring adsorption equilibria is the frontal analysis,[14−16] in which successive step changes of known concentration are introduced at the column inlet and the breakthrough profiles are monitored from the beginning until final concentrations are reached. Such a frontal analysis is usually performed by one of the two following methods: (1) staircase method and (2) step series method.[15] In the former method, the feed concentration is increased stepwise (Figure 1a), whereas in the latter method, the column is equilibrated with pure eluent in between successive concentration steps. Between the two, the staircase method was chosen in this study for determination of adsorption isotherms because of its higher accuracy than the step series method.[15]

For the staircase frontal analysis method, the amount of solutes adsorbed as a result of a step increase in feed concentration can be estimated from the following integral mass balance

(amount of input into the column for Δt) − (amount of output from the column for Δt) = (amount of increase within the column for Δt) (1)

where $\Delta t = t_j - t_{j-1}$; the subscript j indicates the step number; and the time t_0 is set to zero. With an increase in the step number, the column is saturated at increasingly higher concentration, which is equal to the feed concentration applied in each step. The application of the above expression to the first step, which is depicted in Figure 1b, results in

$$C_1 \cdot F \cdot (t_1 - t_0) - F \cdot \int_{t_0}^{t_1} C_{\text{effluent}} \mathrm{d}t = C_1 \cdot (V_0 + V_D) + q_1 \cdot V_S \quad (2)$$

where C_1 is the feed concentration employed during the first step; F is the flow rate; C_{effluent} is the concentration of effluent from the column; V_D is the extra-column dead volume; and q_1 is the solid-phase concentration (i.e., the mass of solutes adsorbed per unit resin volume) in equilibrium with C_1. In addition, V_0 and V_S are the entire void volume and the total solid (or adsorbent) volume within the column, respectively, each of which can be expressed as a function of void fraction and bed volume (BV) as follows

$$V_0 = \text{BV} \cdot [\varepsilon_b + (1 - \varepsilon_b) \cdot \varepsilon_p] \quad (3a)$$

$$V_S = \text{BV} \cdot (1 - \varepsilon_b) \cdot (1 - \varepsilon_p) \quad (3b)$$

where ε_b and ε_p are the interparticle and the intraparticle void fractions, respectively.

In the above derivation, the bed is assumed to be clean at the beginning of the first step, which is mostly accepted in frontal analysis experiments. However, at the beginning of the second step, the bed is no longer clean but saturated at the concentration of C_1 in the mobile phase and q_1 in the solid phase, which comes from the loading during the first step. Considering such an issue and following the same procedures above, one can obtain the following mass balance equation for the second step, which is also described in Figure 1b.

$$C_2 \cdot F \cdot (t_2 - t_1) - F \cdot \int_{t_1}^{t_2} C_{\text{effluent}} \mathrm{d}t = (C_2 - C_1) \cdot (V_0 + V_D) + (q_2 - q_1) \cdot V_S \quad (4)$$

where C_2 is the feed concentration employed during the second step and q_2 is the solid-phase concentration in equilibrium with C_2. Generalization of the above equation to the jth step and its rearrangement leads to

$$q_j = q_{j-1} + \frac{C_j \cdot F \cdot (t_j - t_{j-1}) - F \cdot \int_{t_{j-1}}^{t_j} C_{\text{effluent}} \mathrm{d}t - (C_j - C_{j-1}) \cdot (V_0 + V_D)}{V_S} \quad (5)$$

where C_j is the feed concentration employed during the jth step and q_j is the solid-phase concentration in equilibrium with C_j.

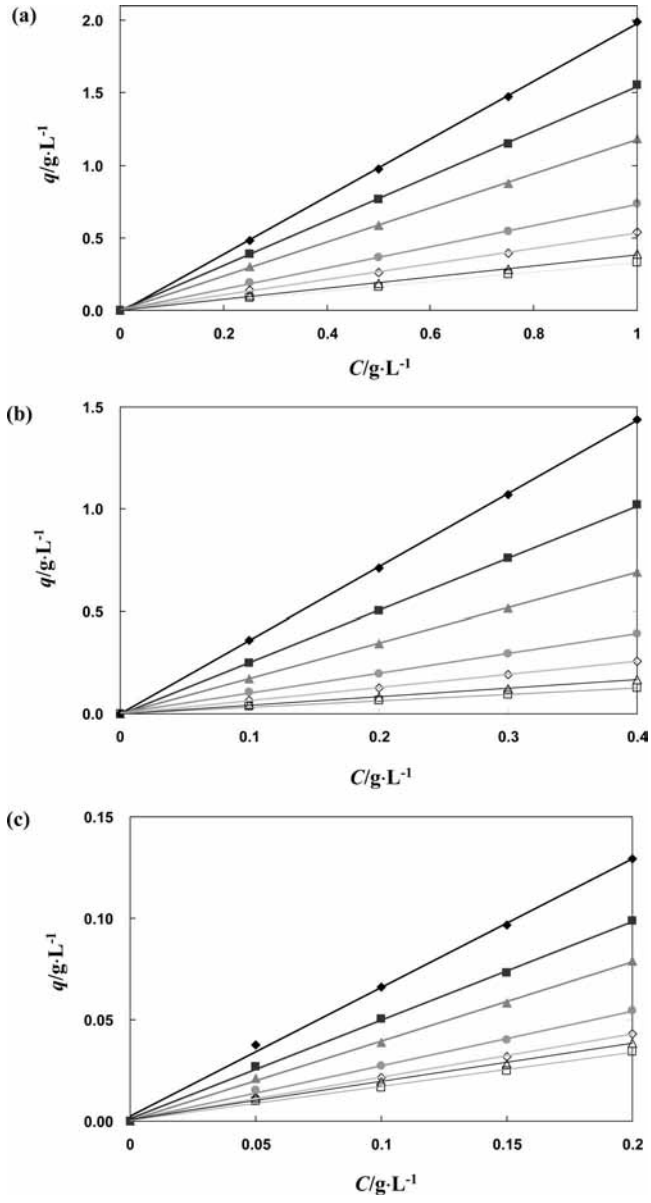

Figure 3. Single-component adsorption equilibria (plot of solid-phase concentration q versus liquid-phase concentration C at equilibrium) of each amino acid in the range of methanol volume fraction $\phi = 0.2$ to 0.7 in the mobile phase. (a) 2-Amino-3-phenylpropanoic acid; (b) 2-amino-3-(3-indolyl)-propanoic acid; (c) 2-amino-3-(4- hydroxyphenyl)-propanoic acid. Symbols: ◆, $\phi = 0.20$; ■, $\phi = 0.25$; ▲, $\phi = 0.30$; ●, $\phi = 0.40$; ◇, $\phi = 0.50$; Δ, $\phi = 0.60$; □, $\phi = 0.70$. Lines calculated from eq 6.

Table 1. Single-Component Adsorption Equilibrium Data for the Case Where the Methanol Volume Fraction ϕ Ranges from 0.2 to 0.7 in the Mobile Phase

2-amino-3-phenyl-propanoic acid		2-amino-3-(3-indolyl)-propanoic acid		2-amino-3-(4-hydroxyphenyl)-propanoic acid	
C/g·L^{-1}	q/g·L^{-1}	C/g·L^{-1}	q/g·L^{-1}	C/g·L^{-1}	q/g·L^{-1}
			$\phi = 0.20$		
0.25	0.4830	0.10	0.3587	0.05	0.0376
0.50	0.9749	0.20	0.7130	0.10	0.0659
0.75	1.4752	0.30	1.0715	0.15	0.0966
1.00	1.9902	0.40	1.4383	0.20	0.1292
			$\phi = 0.25$		
0.25	0.3914	0.10	0.2492	0.05	0.0270
0.50	0.7634	0.20	0.5007	0.10	0.0503
0.75	1.1496	0.30	0.7583	0.15	0.0730
1.00	1.5526	0.40	1.0203	0.20	0.0986
			$\phi = 0.30$		
0.25	0.2989	0.10	0.1736	0.05	0.0212
0.50	0.5845	0.20	0.3419	0.10	0.0388
0.75	0.8772	0.30	0.5140	0.15	0.0581
1.00	1.1816	0.40	0.6919	0.20	0.0790
			$\phi = 0.40$		
0.25	0.1896	0.10	0.1055	0.05	0.0152
0.50	0.3660	0.20	0.1976	0.10	0.0272
0.75	0.5462	0.30	0.2949	0.15	0.0399
1.00	0.7350	0.40	0.3930	0.20	0.0545
			$\phi = 0.50$		
0.25	0.1414	0.10	0.0661	0.05	0.0115
0.50	0.2634	0.20	0.1252	0.10	0.0214
0.75	0.3969	0.30	0.1903	0.15	0.0319
1.00	0.5383	0.40	0.2573	0.20	0.0431
			$\phi = 0.60$		
0.25	0.1031	0.10	0.0437	0.05	0.0117
0.50	0.1848	0.20	0.0808	0.10	0.0195
0.75	0.2835	0.30	0.1229	0.15	0.0283
1.00	0.3911	0.40	0.1690	0.20	0.0386
			$\phi = 0.70$		
0.25	0.0890	0.10	0.0359	0.05	0.0098
0.50	0.1644	0.20	0.0639	0.10	0.0163
0.75	0.2477	0.30	0.0936	0.15	0.0246
1.00	0.3310	0.40	0.1265	0.20	0.03457

From the above equation, one can calculate the value of q_j in equilibrium with the feed concentration of C_j in each step. Such a series of procedures allow a quick and precise measurement of adsorption equilibria.

If the adsorption equilibrium data measured show a linear relationship between q and C, one can use the following isotherm equation to correlate the equilibrium data.

$$q = HC \quad (6)$$

where H is the Henry's constant. In the field of liquid chromatographic research, Henry's constant is defined as the ratio of solid-phase concentration to liquid-phase concentration at equilibrium,[11,17,18] which has often been referred to as partition coefficient.[19]

Physical Models for Describing the Role of Solvent in Liquid Chromatography. To date, two model equations suggested by Snyder[20,21] and Soczewinski[22,23] have been widely used to describe the effect of solvent composition on the adsorption equilibria in liquid chromatography. Both models assume the occurrence of monolayer adsorption and the absence of solute−solvent interactions in mobile and solid phases.[20] The major difference is that the Snyder model assumes a continuous, constant-energy adsorbent surface whereas the Soczewinski model assumes discrete adsorption sites which are not closely spaced—with inactive surface in between these sites.[20]

Table 2. Henry's Constant H, Regression Coefficient R^2, and Standard Deviation σ for the Case Where the Methanol Volume Fraction ϕ Ranges from 0.2 to 0.7 in the Mobile Phase

ϕ	H	R^2	σ^a/g·L^{-1}
	2-amino-3-phenyl-propanoic acid		
0.20	1.9759	0.9998	0.0116
0.25	1.5437	0.9998	0.0079
0.30	1.1768	0.9999	0.0047
0.40	0.7334	0.9998	0.0038
0.50	0.5349	0.9994	0.0051
0.60	0.3850	0.9982	0.0065
0.70	0.3313	0.9994	0.0032
	2-amino-3-(3-indolyl)-propanoic acid		
0.20	3.5841	1.0000	0.0035
0.25	2.5355	0.9998	0.0050
0.30	1.7223	0.9999	0.0025
0.40	0.9857	0.9995	0.0035
0.50	0.6389	0.9996	0.0020
0.60	0.4167	0.9988	0.0023
0.70	0.3169	0.9979	0.0022
	2-amino-3-(4-hydroxyphenyl)-propanoic acid		
0.20	0.6508	0.9972	0.0026
0.25	0.4939	0.9987	0.0014
0.30	0.3927	0.9991	0.0009
0.40	0.2715	0.9981	0.0009
0.50	0.2149	0.9994	0.0004
0.60	0.1932	0.9946	0.0011
0.70	0.1694	0.9955	0.0009

$^a\ \sigma = \sqrt{\sum_{i=1}^{n} (q_i^{cal} - q_i^{exp})^2/(n - p)}$, where q^{cal} and q^{exp} are the calculated solid-phase concentration and the experimentally measured solid-phase concentration, respectively; n is the number of data points ($n = 5$); and p is the number of model parameters fitted ($p = 1$).

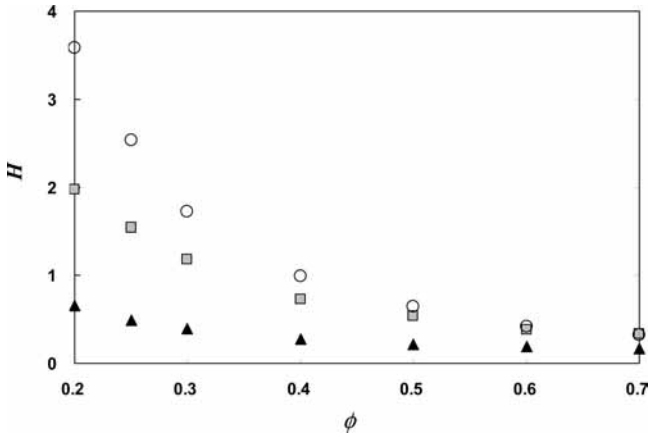

Figure 4. Henry's constant H of each amino acid as a function of methanol volume fraction ϕ in the mobile phase. ▲, 2-amino-3-(4-hydroxyphenyl)-propanoic acid; ■, 2-amino-3-phenyl-propanoic acid; ○, 2-amino-3-(3-indolyl)-propanoic acid.

Their model equations, which were originally derived as a function of capacity factor and solvent composition, have often been expressed in terms of Henry's constant and solvent composition in the literature.[11,18] The model equations based on such an expression are given by

$$H = f_1 \cdot \exp(-f_2 \cdot \phi) \tag{7a}$$

for the Snyder model and

$$H = (f_1 \cdot \phi)^{-f_2} \tag{7b}$$

for the Soczewinski model where H is the Henry's constant; f_1 and f_2 are the model parameters; and ϕ is the volume fraction of an organic solvent in the mobile phase. Although the model parameters (f_1 and f_2) have their own physical significances, they have mostly functioned as empirical parameters for fitting experiment data in previous studies.[11,18,24]

Table 3. Snyder and Soczewinski Model Parameters f_1 and f_2 Resulting from Fitting the Model Equations (Equations 7a and 7b) to the Experimentally Determined Henry's Constants in the Range of Methanol Volume Fraction $\phi = 0.2$ to 0.7 in the Mobile Phase

Snyder model			Soczewinski model		
f_1	f_2	σ^a	f_1	f_2	σ^a
2-Amino-3-phenyl-propanoic acid					
3.6568	3.6587	0.1211	3.0619	1.4845	0.0540
2-Amino-3-(3-indolyl)-propanoic acid					
8.0896	4.8713	0.2686	2.5465	1.9718	0.1008
2-Amino-3-(4-hydroxyphenyl)-propanoic acid					
0.9235	2.6352	0.0570	7.7409	1.0891	0.0186

$^a\ \sigma = \sqrt{\sum_{i=1}^{n} (H_i^{cal} - H_i^{exp})^2/(n - p)}$, where H^{cal} and H^{exp} are the model-predicted Henry's constant and the experimentally determined Henry's constant, respectively; n is the number of data points ($n = 7$); and p is the number of model parameters fitted ($p = 2$).

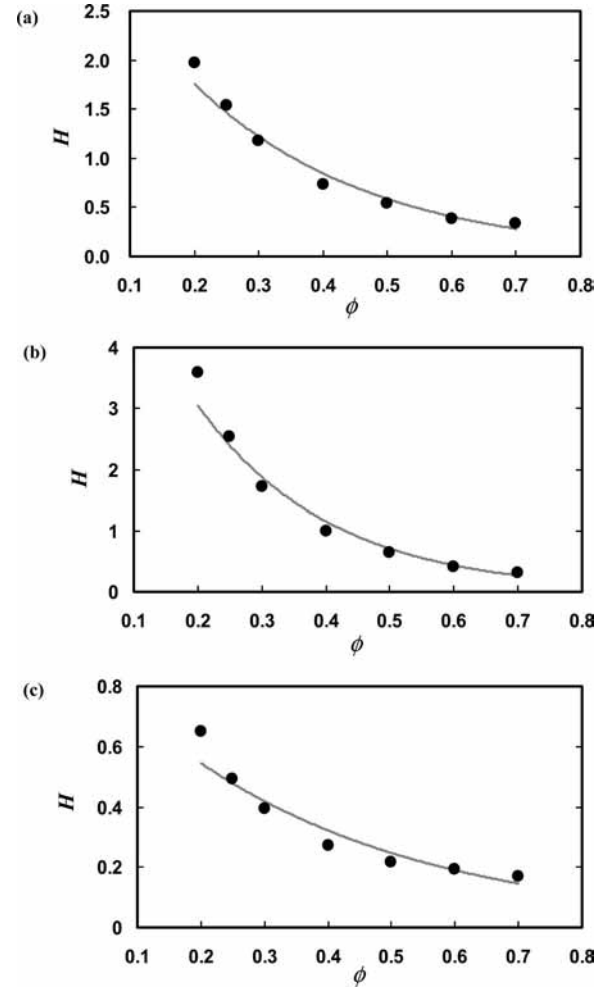

Figure 5. Comparison of the experimentally determined Henry's constants H (symbol: ●) and the predicted Henry's constants H (line: —) from the Snyder model for the case where the methanol volume fraction $\phi = 0.2$ to 0.7 in the mobile phase. (a) 2-Amino-3-phenyl-propanoic acid; (b) 2-amino-3-(3-indolyl)-propanoic acid; (c) 2-amino-3-(4-hydroxyphenyl)-propanoic acid.

Experimental Section

Materials. The amino acids under investigation included (*S*)-2-amino-3-phenyl-propanoic acid (99 %), (*S*)-2-amino-3-(3-indolyl)-propanoic acid (98 %), and (*S*)-2-amino-3-(4-hydroxyphenyl)-propanoic acid (99 %), all of which were purchased from Sigma-Aldrich Co. (St. Louis, MO). Blue dextran and sodium chloride, which were used as tracer molecules for the

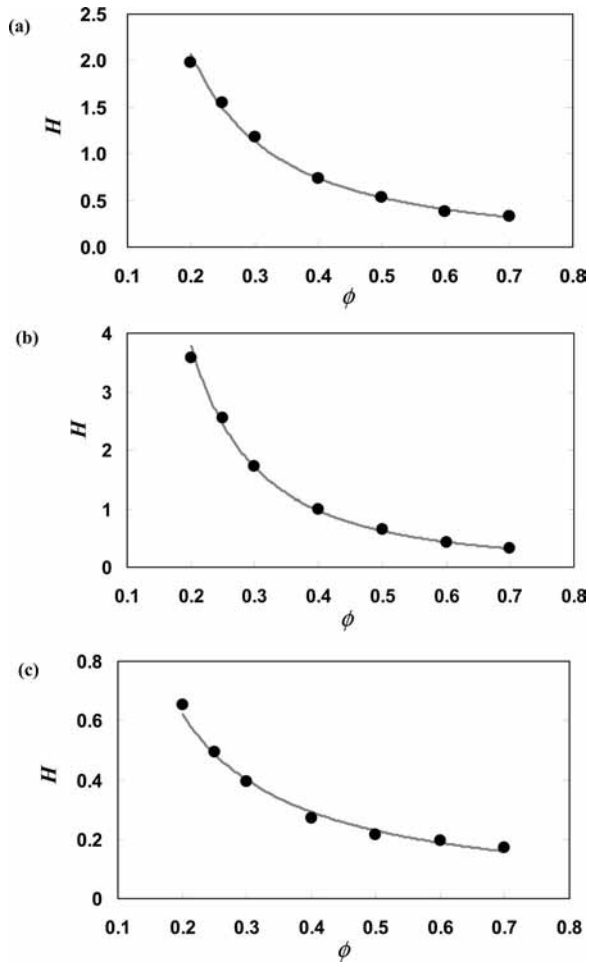

Figure 6. Comparison of the experimentally determined Henry's constants H (symbol: ●) and the predicted Henry's constants H (line: —) from the Soczewinski model for the case where the methanol volume fraction ϕ = 0.2 to 0.7 in the mobile phase. (a) 2-Amino-3-phenyl-propanoic acid, (b) 2-amino-3-(3-indolyl)-propanoic acid; (c) 2-amino-3-(4-hydroxyphenyl)-propanoic acid.

Table 4. Single-Component Adsorption Equilibrium Data for the Case Where the Methanol Volume Fraction ϕ Ranges from 0.05 to 0.15 in the Mobile Phase

2-amino-3-phenyl-propanoic acid		2-amino-3-(3-indolyl)-propanoic acid		2-amino-3-(4-hydroxyphenyl)-propanoic acid	
C/g·L^{-1}	q/g·L^{-1}	C/g·L^{-1}	q/g·L^{-1}	C/g·L^{-1}	q/g·L^{-1}
			ϕ = 0.05		
0.25	1.6186	0.10	1.5706	0.05	0.1118
0.50	3.1421	0.20	3.1558	0.10	0.2112
0.75	4.7178	0.30	4.7796	0.15	0.3076
1.00	6.3458	0.40	6.4190	0.20	0.4025
			ϕ = 0.10		
0.25	1.0176	0.10	0.9051	0.05	0.0711
0.50	1.9852	0.20	1.7902	0.10	0.1303
0.75	2.9535	0.30	2.6832	0.15	0.1855
1.00	3.9465	0.40	3.5651	0.20	0.2478
			ϕ = 0.15		
0.25	0.7186	0.10	0.5593	0.05	0.0525
0.50	1.3864	0.20	1.1068	0.10	0.0964
0.75	2.0729	0.30	1.6641	0.15	0.1414
1.00	2.7483	0.40	2.2000	0.20	0.1870

measurement of column void fraction, were also purchased from Sigma-Aldrich Co. (St. Louis, MO). Methanol was obtained from Mallinckrodt Baker, Inc. (Paris, KY) and used as an organic solvent in the mobile phase employed. The mobile phase was prepared by mixing methanol and deionized distilled water (DDW).

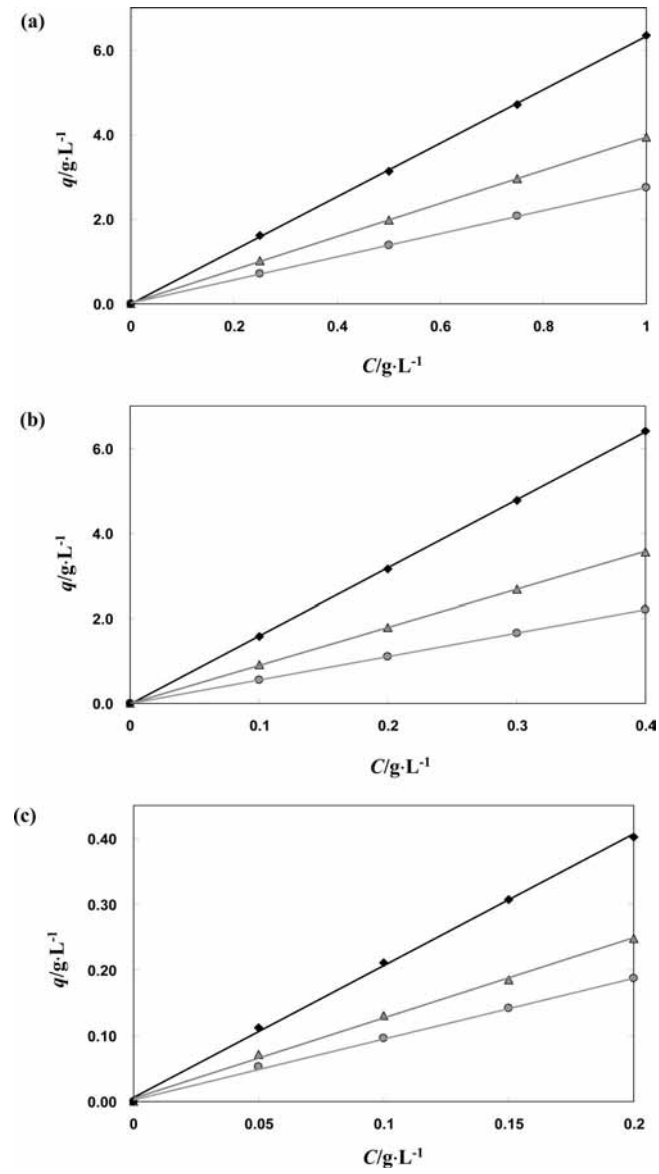

Figure 7. Single-component adsorption equilibria (plot of solid-phase concentration q versus liquid-phase concentration C at equilibrium) of each amino acid in the range of methanol volume fraction ϕ = 0.05 to 0.15 in the mobile phase. (a) 2-Amino-3-phenyl-propanoic acid; (b) 2-amino-3-(3-indolyl)-propanoic acid; (c) 2-amino-3-(4-hydroxyphenyl)-propanoic acid. Symbols: ◆, ϕ = 0.05; ▲, ϕ = 0.10; ●, ϕ = 0.15. Lines calculated from eq 6.

Apparatus. The experiments were conducted with the HPLC system (Figure 2), which consisted of two HPLC pumps (Waters 515), a PDA detector (Waters 996), and an injector (Rheodyne 9725i). The experimental data from the HPLC system were collected and analyzed with the help of Waters Millennium software operating in the Windows environment. A Capcell Pak C_{18} resin with an average particle size of 20 μm was used as the adsorbent of this study. The column containing the resin has a length of 250 mm and a diameter of 10 mm, and it was prepacked by the manufacturer (Shiseido Co. in Japan). A Milli-Q system by Millipore (Bedford, MA) was used to obtain DDW.

Methods. To check the effect of mobile-phase composition on the adsorption equilibria, the percentage of organic solvent, i.e., methanol in the mobile phase, was varied in each experiment. The range of methanol percentage in the mobile phase employed was from 20 % to 70 % by volume in the first set of

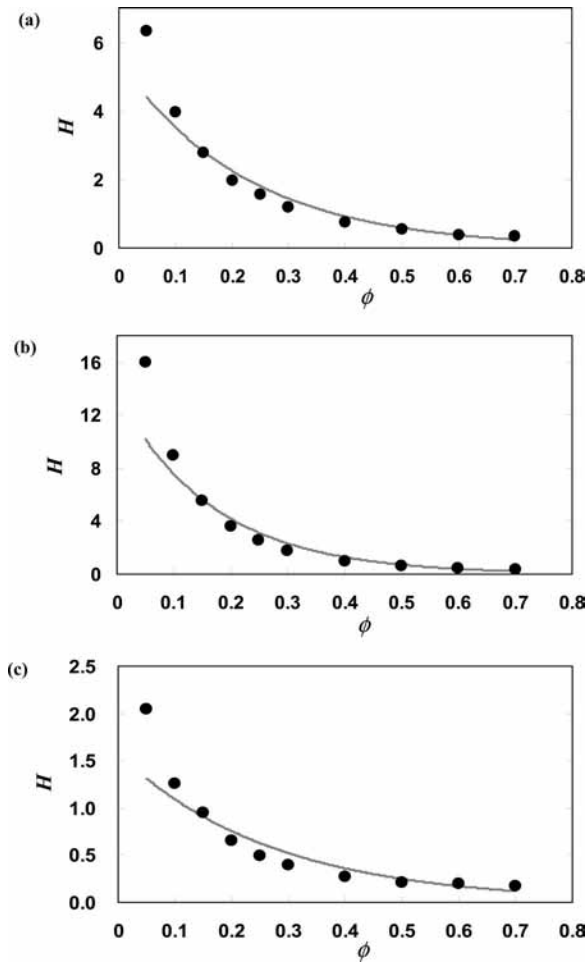

Figure 8. Comparison of the experimentally determined Henry's constants H (symbol: ●) and the predicted Henry's constants H (line: —) from the Snyder model for the case where the methanol volume fraction $\phi = 0.05$ to 0.7 in the mobile phase. (a) 2-Amino-3-phenyl-propanoic acid; (b) 2-amino-3-(3-indolyl)-propanoic acid; (c) 2-amino-3-(4-hydroxyphenyl)-propanoic acid.

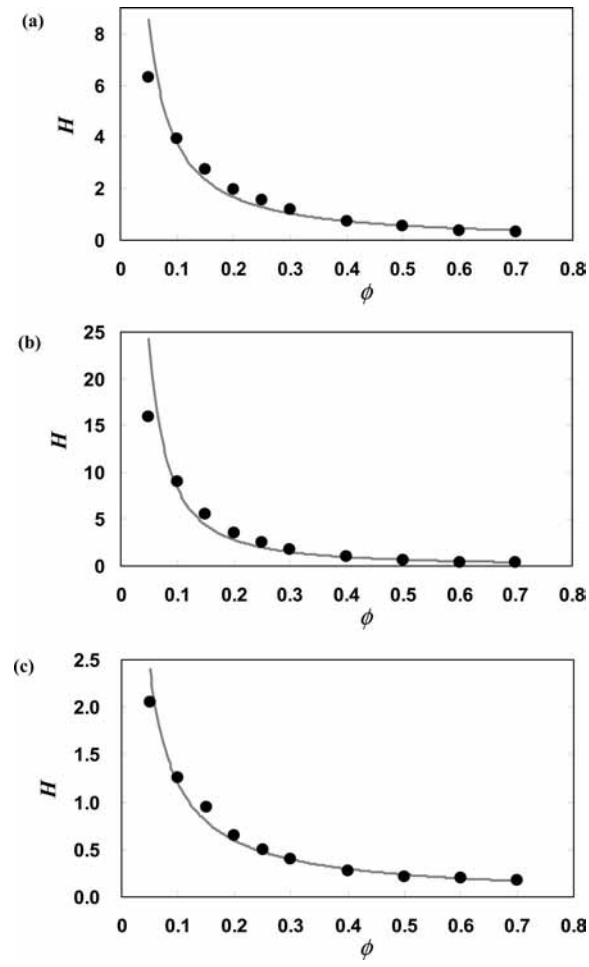

Figure 9. Comparison of the experimentally determined Henry's constants H (symbol: ●) and the predicted Henry's constants H (line: —) from the Soczewinski model for the case where the methanol volume fraction $\phi =$ 0.05 to 0.7 in the mobile phase. (a) 2-Amino-3-phenyl-propanoic acid; (b) 2-amino-3-(3-indolyl)-propanoic acid; (c) 2-amino-3-(4-hydroxyphenyl)-propanoic acid.

Table 5. Henry's Constant H, Regression Coefficient R^2, and Standard Deviation σ for the Case Where the Methanol Volume Fraction ϕ Ranges from 0.05 to 0.15 in the Mobile Phase

ϕ	H	R^2	σ^a/g·L^{-1}
	2-Amino-3-phenyl-propanoic acid		
0.05	6.3253	0.9999	0.0270
0.10	3.9512	0.9999	0.0116
0.15	2.7605	0.9998	0.0159
	2-Amino-3-(3-indolyl)-propanoic acid		
0.05	15.966	0.9999	0.0285
0.10	8.9318	1.0000	0.0075
0.15	5.5217	0.9999	0.0069
	2-Amino-3-(4-hydroxyphenyl)-propanoic acid		
0.05	2.0466	0.9982	0.0067
0.10	1.2528	0.9970	0.0053
0.15	0.9448	0.9984	0.0030

[a] The standard deviation (σ) was estimated as described in the footnote of Table 2.

experiments. Its range was then extended from 5 % to 70 % by volume. Two different types of chromatographic experiments were conducted, which included pulse injection experiments (or pulse tests) and staircase frontal experiments (or staircase frontal tests). All of these experiments were carried out at room temperature. Extra-column dead volume was measured by a pulse or a single frontal test without the column after each chromatographic experiment.

To perform pulse tests, a sampling loop was connected to the injector (Figure 2a). In the load position, the loop was filled with a feed solution. The eluent flow rate was controlled by the Millennium software. Then the injection valve was switched to the inject position to start the injection. Data recording was started simultaneously. Two pulse tests were carried out with blue dextran (1 g·L^{-1}) and sodium chloride (0.5 M), respectively. Their loading volumes through the column were (50 and 20) μm, respectively. The effluent concentration was detected by the PDA detector at the wavelengths of 254 nm for blue dextran and 210 nm for sodium chloride.

For staircase frontal tests, both HPLC pumps were used (Figure 2b). One pump delivered mobile-phase solution and the other feed solution (amino acid solution). The feed concentration was kept constant throughout the experiments as follows: (*S*)-2-amino-3-phenyl-propanoic acid (1 g·L^{-1}), (*S*)-2-amino-3-(3-indolyl)-propanoic acid (0.4 g·L^{-1}), and (*S*)-2-amino-3-(4-hydroxyphenyl)-propanoic acid (0.2 g·L^{-1}). The two streams were mixed before entering the column. Such a mixing process was facilitated using a Dynamax dual chamber mixer (Varian 0.6 ML SS), which enabled the two streams to attain the state of a perfect mixing before entering the column. The total flow rate for the mixed stream was kept constant at 2 mL·min^{-1}. Various feed compositions (25 %, 50 %, 75 %, and 100 %) were obtained by changing the ratio of the two streams. The

Table 6. Snyder, Soczewinski, and Abel Model Parameters f_1, f_2, and f_3 Resulting from Fitting the Model Equations (Equations 7a, 7b, and 9) to the Experimentally Determined Henry's Constants in the Range of Methanol Volume Fraction $\phi = 0.05$ to 0.7 in the Mobile Phase

Snyder model			Soczewinski model			Abel model			
f_1	f_2	σ^a	f_1	f_2	σ^a	f_1	f_2	f_3	σ^a
2-Amino-3-phenyl-propanoic acid									
5.4888	4.4646	0.7238	3.2330	1.1773	0.8156	12.5677	9.1504	1.7893	0.0618
2-Amino-3-(3-indolyl)-propanoic acid									
3.6427	5.9076	2.1460	2.5618	1.5526	3.0020	32.8282	5.3444	3.0385	0.0391
2-Amino-3-(4-hydroxyphenyl)-propanoic acid									
1.5771	3.6928	0.2796	8.3751	1.0088	0.1414	4.0394	10.8457	1.5703	0.0313

[a] $\sigma = \sqrt{\sum_{i=1}^{n} (H_i^{cal} - H_i^{exp})^2/(n - p)}$, where H^{cal} and H^{exp} are the model-predicted Henry's constant and the experimentally determined Henry's constant, respectively; n is the number of data points ($n = 10$); and p is the number of model parameters fitted ($p = 2$ for Snyder and Soczewinski models; $p = 3$ for Abel model).

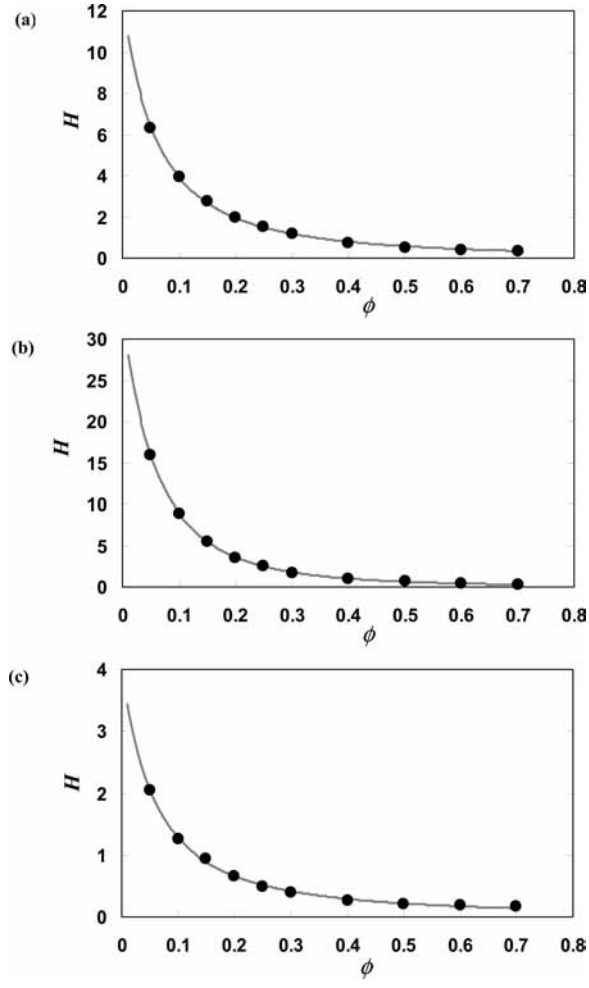

Figure 10. Comparison of the experimentally determined Henry's constants H (symbol: ●) and the predicted Henry's constants H (line: —) from Abel's model for the case where the methanol volume fraction $\phi = 0.05$ to 0.7 in the mobile phase. (a) 2-Amino-3-phenyl-propanoic acid; (b) 2-amino-3-(3-indolyl)-propanoic acid; (c) 2-amino-3-(4-hydroxyphenyl)-propanoic acid.

ratio was changed only after a concentration plateau was fully developed at the column outlet. The column effluent was monitored at the wavelengths of 254 nm for (*S*)-2-amino-3-phenyl-propanoic acid, 300 nm for (*S*)-2-amino-3-(3-indolyl)-propanoic acid, and 260 nm for (*S*)-2-amino-3-(4-hydroxyphenyl)-propanoic acid using the PDA detector.

Results and Discussion

Pulse Tests for Estimation of Interparticle and Intraparticle Void Fractions. Column void fraction is one of the important parameters needed for estimating adsorption equilibria from a frontal analysis method, as mentioned in the theory section. The void fraction to be determined for such a purpose includes interparticle (ε_b) and intraparticle void fractions (ε_p), as can be seen in eq 3a.

One of the effective ways of estimating the void fractions is to inject a pulse of nonretained tracer molecule through a column and measure its elution volume (that is, the volume of effluent at which the tracer molecule exits from the column).

For the estimation of interparticle void fraction, a pulse test was conducted with blue dextran, which is totally excluded from the resin particles because the blue dextran molecule is much larger than the resin pore size and nonadsorbed onto the resin particles. Therefore, the elution volume of a blue dextran pulse is virtually equal to the interparticle void volume. Dividing such an interparticle volume by bed volume resulted in the interparticle void fraction, which was estimated to be 0.30 for the chromatographic column employed in this study.

Unlike the case of interparticle void fraction above, the estimation of intraparticle void fraction began with the measurement of total void volume instead of its corresponding void volume, i.e., intraparticle void volume. The total void volume was measured from the elution volume of a sodium chloride pulse because the sodium chloride molecule is sufficiently small to penetrate the entire intraparticle space while nonadsorbed onto the resin particles. Subtracting the aforementioned interparticle void volume from the total void volume, one can obtain the intraparticle volume. Division of such an intraparticle void volume by the total solid (or adsorbent) volume resulted in the intraparticle void fraction, which was estimated to be 0.50 for the adsorbent employed in this study.

Staircase Frontal Tests for the Measurement of Adsorption Equilibria. Table 1 presents the single-component adsorption data of 2-amino-3-phenyl-propanoic acid, 2-amino-3-(3-indolyl)-propanoic acid, and 2-amino-3-(4-hydroxyphenyl)-propanoic acid on the Capcell pack C_{18} resin, which were measured using the staircase frontal analysis method while varying the methanol content in the mobile phase from 20 % (v/v) to 70 % (v/v). To analyze the pattern of such adsorption data (Table 1), the solid-phase and liquid-phase concentrations at equilibrium (q and C) are plotted in Figure 3. It is easily seen that the adsorption pattern of each amino acid component follows a linear isotherm relation in the investigated range of mobile-phase composition. Under such circumstances, a set of adsorption equilibrium data can be characterized by Henry's constant, which is the ratio of solid-phase concentration to liquid-phase concentration at equilibrium.

Henry's constant was obtained for each mobile-phase composition by using linear regression based on a least-squares analysis, and the resultant value is summarized in Table 2 together with its related regression coefficient, R^2.

The above Henry's constant value and a linear isotherm equation (eq 6) were used to calculate the solid-phase concentrations in equilibrium with liquid-phase concentrations. The calculation results are compared with the experimental data in Figure 3, which shows a close agreement between them. In addition, the standard deviations between the experimentally measured solid-phase concentrations and the calculated solid-phase concentrations were estimated, and they are listed in Table 2. The standard deviation values (Table 2), the regression coefficient values (Table 2), and the comparison result (Figure 3) indicate that a linear isotherm equation can be the most reliable one in describing the adsorption equilibria of each amino acid on the Capcell pack C_{18} resin in its investigated range of concentrations.

Henry's constants of the three amino acids, which were determined in this section, are all plotted in Figure 4. Note that the Henry's constant of 2-amino-3-(3-indolyl)-propanoic acid was highest while that of 2-amino-3-(4-hydroxyphenyl)-propanoic acid was lowest. Another noteworthy observation in Figure 4 is that the Henry's constant of each component has a decreasing trend as the methanol content in the mobile phase increases. This phenomenon is mostly due to a change in the polarity of mobile-phase solution, which is virtually associated with a change in the methanol content. In general, the elution of mobile phase with a lower polarity tends to reduce the adsorption affinity of a solute, i.e., the Henry's constant of a solute in reversed-phase chromatography. In the system of our interest, an increase in the methanol content reduces the polarity of the mobile phase, thus leading to a decrease in the Henry's constant.

Correlation of Henry's Constants as a Function of Mobile-Phase Composition Using the Snyder and Soczewinski Models. Henry's constants reported above for different mobile-phase compositions were fitted with two physical models in this section. The models used are the Snyder and Soczewinski models, each of which has two parameters (f_1 and f_2) to be determined from the comparison with experimental data.

To facilitate the process of determining the parameters of interest, the two model equations (eqs 7a and 7b) are rearranged into the following forms that can allow the use of linear regression based on a least-squares method.

$$\{\ln H\} = \ln f_1 - f_2 \cdot \{\phi\} \tag{8a}$$

for the Snyder model and

$$\{\ln H\} = -f_2 \cdot \ln f_1 - f_2 \cdot \{\ln \phi\} \tag{8b}$$

for the Soczewinski model where the collective bracket { } stands for a set of experimental data and ϕ is the volume fraction of methanol in the mobile phase. The Snyder model parameters were determined through the slope and *y*-intercept, which resulted from the linear regression of $\{\phi\}$ versus $\{\ln H\}$. In the same manner, the Soczewinski model parameters were obtained from the linear regression of $\{\ln \phi\}$ versus $\{\ln H\}$. The resulting parameter values for the two models are listed in Table 3.

The parameter values in Table 3 were then plugged into the model equations, which were used to predict the Henry's constant of each amino acid as a function of mobile-phase composition. The model-predicted results are compared with the experimentally determined Henry's constants in Figures 5 and 6. Notice that the Soczewinski model fits the experimental results better than the Snyder model, which can also be confirmed quantitatively from the standard deviations between the experimental and the model-predicted Henry's constants, as listed in Table 3. Since the Soczewinski model with its related parameter values describes the adsorption equilibrium data with reasonable accuracy, it can play an important role in the design equation for a solvent gradient SMB based on Capcell Pak C_{18} media. One such example is that the Soczewinski model equation and its related parameters can be used to predict the Henry's constant of each amino acid at every location in the SMB packed with Capcell Pak C_{18} media, in which the methanol content varies continuously along the bed.

Additional Adsorption Equilibrium Data Measured under the Condition of Low Methanol Content in the Mobile Phase. In the previous section, the adsorption equilibria of the three amino acids were measured in the range of methanol percentage from 20 % to 70 % in the mobile phase. Although the results demonstrated a marked difference between the highest Henry's constant and the lowest one, such a difference sometimes needs to be enlarged further if the advantage of a solvent gradient operation in SMB is to be fully attained.

To obtain the adsorption equilibrium data with a wider range of Henry's constant, additional experiments were carried out in the range of methanol percentage from 5 % to 15 % in the mobile phase. Table 4 lists the resulting adsorption data, which exhibit a linear isotherm relation as can be seen in Figure 7. The resulting Henry's constant and the related regression coefficients (R^2) are presented in Table 5 together with the standard deviations between the experimental and the calculated solid-phase concentration.

Henry's constants determined in this section were combined with the previous ones (based on the range of methanol percentage from 20 % to 70 % in the mobile phase), and the combined results were attempted to be fitted with the Snyder and Soczewinski models each. However, the two models could not describe the combined results with reasonable accuracy as shown in Figures 8 and 9.

Several other models were tested to find out a proper model for the entire Henry's constant results. It was found that the following model equation containing three parameters (f_1, f_2, and f_3), which was reported by Abel et al.,[12] could fit our results well.

$$H = \frac{f_1}{(1 + f_2 \cdot \phi)^{f_3}} \tag{9}$$

Like in the previous cases, the above three parameters (f_1, f_2, and f_3) were determined by a least-squares fitting of the model equation to the experimentally determined Henry's constants. Since it is impossible to rearrange the above model equation into a linear form, the least-squares fitting process was performed with a well-known optimization program instead of a linear regression method. In this study, a genetic algorithm,[25] which has been known as a highly efficient optimization tool, was employed to minimize the sum $\sum_j (H_j^{\mathrm{exp}} - H_j^{\mathrm{cal}})^2$. The resulting parameter values from the optimization are listed in Table 6 and used to generate the model-predicted Henry's constant curves in the investigated range of methanol content. The model-predicted results are then compared with the experimentally determined Henry's constants. As shown in Figure 10, the two results are in close agreement, indicating that Abel's model can be the most adequate model in describing the entire Henry's constant acquired from our research.

Conclusions

A frontal column experiment, which is one of the dynamic chromatographic methods, was conducted to measure the adsorption equilibria of 2-amino-3-phenyl-propanoic acid,

2-amino-3-(3-indolyl)-propanoic acid, and 2-amino-3-(4-hydroxyphenyl)-propanoic acid on the Capcell Pak C_{18} resin. This experiment was repeated while varying the mobile-phase composition, i.e., the methanol content in the mobile phase. For each mobile-phase condition, Henry's constants were determined from the experimentally measured adsorption data. It was found that the Henry's constant of 2-amino-3-(3-indolyl)-propanoic acid was highest while that of 2-amino-3-(4-hydroxyphenyl)-propanoic acid was lowest. In addition, the Henry's constant of each amino acid exhibited a significant dependence on the mobile-phase composition. Several models were used to correlate the Henry's constant as a function of mobile-phase composition. Among the models used, the Snyder and Soczewinski models failed in such a correlation task. On the other hand, the Abel model was successful in predicting accurately the Henry's constant as a function of mobile-phase composition. The data and model parameters reported in this study can serve as key information in the stage of designing a solvent gradient SMB process for amino acids separation.

Literature Cited

(1) Wu, D. J.; Xie, Y.; Wang, N. H. L. Design of Simulated Moving Bed Chromatography for Amino Acid Separations. *Ind. Eng. Chem. Res.* **1998**, *37*, 4023–4035.

(2) Fennema, O. R. *Food Chemistry*; Marcel Dekker: New York, 1996.

(3) Harper, A. E. *Sweetners: Issues and Uncertainties*; National Academy of Science: WA, 1975.

(4) Fettneto, A. G.; Melanson, S. J.; Nicholson, S. A.; Pennigton, J. J.; Dicosmo, F. Improved Taxol Yield by Aromatic Carboxylic-Acid and Amino-Acid Feeding to Cell-Cultures of Taxus-Cuspidate. *Biotechnol. Bioeng.* **1994**, *44*, 967–971.

(5) Hartmann, E. Effects of L-tryptophan on Sleepiness and on Sleep. *J. Psychiatric Res.* **1983**, *17*, 107–113.

(6) Thomson, J.; Rankin, H.; Ashcroft, G. W.; Yates, C. M.; McQueen, J. K.; Cummings, S. W. The Treatment of Depression in General Practice: a Comparison of L-Tryptophan, Amitriptyline, and a Combination of L-Tryptophan and Amitriptyline with Placebo. *Psychological Med.* **1982**, *12*, 741–751.

(7) Rasmussen, D. D.; Ishizuka, B.; Quigley, M. E.; Yen, S. S. Effects of Tyrosine and Tryptophan Ingestion on Plasma Catecholamine and 3,4-Dihydroxyphenylacetic Acid Concentrations. *J. Clin. Endocrinol. Metab.* **1983**, *57*, 760–763.

(8) Dechow, F. J. *Separation and Purification Techniques in Biotechnology*; Noyes Publications: Park Ridge, 1989.

(9) Jupke, A.; Epping, A.; Schmidt, H. Optimal Design of Batch and Simulated Moving Bed Chromatographic Separation Processes. *J. Chromatogr. A* **2002**, *944*, 93–117.

(10) Xie, Y.; Hritzko, B.; Chin, C. Y.; Wang, N. H. L. Separation of FTC-Ester Enantiomers Using a Simulated Moving Bed. *Ind. Eng. Chem. Res.* **2003**, *42*, 4055–4067.

(11) Antos, D.; Seidel-Morgenstern, A. Application of Gradients in the Simulated Moving Bed Process. *Chem. Eng. Sci.* **2001**, *56*, 6667–6682.

(12) Abel, S.; Mazzotti, M.; Morbidelli, M. Solvent Gradient Operation of Simulated Moving Beds: I. Linear Isotherms. *J. Chromatogr. A* **2002**, *944*, 23–39.

(13) Ohtsu, Y.; Shiojima, Y.; Okumura, T.; Koyama, J. I.; Nakamura, K.; Nakata, O. Performance of Polymer-Coated Silica C18 Packing Materials Prepared from High-Purity Silica Gel. *J. Chromatogr.* **1989**, *48*, 147–157.

(14) Guiochon, G.; Shirazi, S. G.; Katti, A. M. *Fundamentals of Preparative and Nonlinear Chromatography*; Academic Press: New York, 1994.

(15) Vente, J. A.; Bosch, H.; de Haan, A. B.; Bussmann, P. J. T. Evaluation of Sugar Sorption Isotherm Measurement by Frontal Analysis under Industrial Processing Conditions. *J. Chromatogr. A* **2005**, *1066*, 72–79.

(16) Zhang, Y.; Hidajat, K.; Ray, A. K. Determination of Competitive Adsorption Isotherm Parameters of Pindolol Enantiomers on α_1-Aicd Glycoprotein Chiral Stationary Phase. *J. Chromatogr. A* **2006**, *1131*, 176–184.

(17) Bae, Y. S.; Lee, C. H. Partial-Discarded Strategy for Obtaining High Purity Products Using Simulated Moving Bed Chromatography. *J. Chromatogr. A* **2006**, *1122*, 161–173.

(18) Ziomek, G.; Kaspereit, M.; Jezowski, J.; Seidel-Morgenstern, A.; Antos, D. Effect of Mobile Phase Composition on the SMB Process Efficiency: Stochastic Optimization of Isocratic and Gradient Operation. *J Chromatogr. A* **2005**, *1070*, 111–124.

(19) Xie, Y.; Wu, D.; Ma, Z.; Wang, N. H. L. Extended Standing Wave Design Method for Simulated Moving Bed Chromatography: Linear Systems. *Ind. Eng. Chem. Res.* **2000**, *39*, 1993–2005.

(20) Snyder, L. R. Role of the Solvent in Liquid-Solid Chromatography—A review. *Anal. Chem.* **1974**, *46*, 1384–1393.

(21) Snyder, L. R.; Dolan, J. W.; Gant, J. R. Gradient Elution in High-Performance Liquid Chromatography. *J. Chromatogr.* **1979**, *165*, 3–30.

(22) Soczewinski, E. Solvent Composition Effects in Thin-Layer Chromatography Systems of the Type Silica Gel-Electron Donor Solvent. *Anal. Chem.* **1969**, *41*, 179–182.

(23) Soczewinski, E.; Golkiewicz, W. A. A Simple Molecular Model for Adsorption Chromatography. VII Relationship between the R_M Value and the Composition for Phenols in Systems of the Type (Cyclohexane+Polar Solvent)/Silica. *Chromatographia* **1973**, *6*, 269–273.

(24) Wu, D. J.; Ma, Z.; Wang, N. H. L. Optimization of Throughput and Desorbent Consumption in Simulated Moving Bed Chromatography for Paclitaxel Purification. *J. Chromatogr. A* **1999**, *855*, 71–89.

(25) Kasat, R. B.; Gupta, S. K. Multi-Objective Optimization of an Industrial Fluidized-Bed Catalytic Cracking unit (FCCU) Using Genetic Algorithm (GA) with the Jumping Genes Operator. *Comput. Chem. Eng.* **2003**, *27*, 1785–1800.

Received for review July 3, 2008. Accepted August 29, 2008. This work was supported by the research fund of Hanyang University (HY-2007-S).

JE800510Y